

Plasmonic modification of electron-longitudinal-optical phonon coupling in Ag-nanoparticle embedded InGaN/GaN quantum wells

Antonio Llopis, Sérgio M. S. Pereira, Ian M. Watson, and Arup Neogi*

Citation: *Appl. Phys. Lett.* **105**, 091103 (2014); doi: 10.1063/1.4894371

View online: <http://dx.doi.org/10.1063/1.4894371>

View Table of Contents: <http://aip.scitation.org/toc/apl/105/9>

Published by the [American Institute of Physics](#)

Fearful for the future of science?

Programs and Resources | Publications | Career Resources | Member Societies | About AIP | [Contact Us](#)

FYI
FOR YOUR INFORMATION

on authoritative news and resources

FYI This Week
A free e-newsletter, issued each Monday morning and covers the week's news and events of the physics community.

The Week's Top
A weekly digest of the week's top news stories, research highlights, and career opportunities.

Sign up for FREE FYI emails.
AIP | American Institute of Physics

FYI Bulletin

Plasmonic modification of electron-longitudinal-optical phonon coupling in Ag-nanoparticle embedded InGaN/GaN quantum wells

Antonio Llopis,¹ Sérgio M. S. Pereira,² Ian M. Watson,³ and Arup Neogi^{1,a)}

¹*Department of Physics, University of North Texas, Denton, Texas 76203, USA*

²*Department of Physics, CICECO, Universidade de Aveiro, 3810 193 Aveiro, Portugal*

³*Institute of Photonics, University of Strathclyde, Wolfson Centre, 106 Rottenrow East, Glasgow G4 0NW, United Kingdom*

(Received 10 June 2014; accepted 16 August 2014; published online 2 September 2014)

Surface plasmon enhanced GaN and InGaN quantum wells (QWs) show promise for use as room-temperature light emitters. The effectiveness of the plasmon enhancement, however, is limited by the strong electron/hole and longitudinal optical phonon coupling found in the III-V nitrides. The electron-phonon coupling within semiconductor QWs has been modified using silver nanoparticles embedded within the QWs. Direct evidence is provided for this change via confocal Raman spectroscopy of the samples. This evidence is augmented by Angle-dependent photoluminescence experiments which show the alteration of the electron-phonon coupling strength through measurement of the emitted phonon replicas. Together these demonstrate a direct modification of carrier-phonon interactions within the system, opening up the possibility of controlling the coupling strength to produce high-efficiency room-temperature light emitters. © 2014 AIP Publishing LLC.

[<http://dx.doi.org/10.1063/1.4894371>]

The optical properties of confined excitons or carriers in III-nitrides alloys and quantum well (QW) based devices such as ultraviolet (UV)-visible lasers, light emitting diodes (LEDs), solar blind ultraviolet detectors, and high power optoelectronic devices are influenced by longitudinal phonon scattering. Due to the large longitudinal-optical (LO) phonon (LOP) energy of InN (86 meV) and GaN (91 meV), the strength of the interaction of the carriers or excitons with the phonons affects the interband and intersubband optical transitions in these structures. There has been increased interest in realizing white light emitters and photovoltaic devices using nitride semiconductors that have a bandgap spanning from the UV to the near-infrared wavelength regime. GaN and its tertiary compounds have been utilized for realizing efficient UV¹ and visible LEDs.² Radiative recombination of excitons in semiconductors is accompanied by phonon (ph) replicas (PR) which influence the absorption and emission efficiency of the nitride based devices.³ The large LO phonon energy should minimize non-radiative intersubband transitions due to low emission probability of LO phonons.³ The strength of exciton-phonon coupling also provides useful information about an indirect Auger recombination process due to scattering, which plays a major role in efficiency droop in nitride based emitters.⁴

Surface plasmon (SP) induced enhancement of light emission in nitrides is a potentially attractive way of increasing the efficiency of nitride LEDs due to the enhancement of the radiative recombination rate. The coupling between LOP and exciton, which has been studied extensively using photoluminescence (PL) measurements on III-nitrides, has not yet been investigated in nitride-based plasmonic light emitters. Long range plasmons are normally dissipative due to the resonant coupling of the excitons or free carriers to the surface

plasmon modes. A study of the exciton-phonon coupling mechanism in plasmonic light emitters and its role in the light emission efficiency can result in designing more efficient room-temperature nitride based light emitters. Long range SP mediated recombination at room temperature is generally dominated by non-radiative recombination process yielding very low internal quantum efficiencies. One possible means of bypassing this issue would be to directly modify the electron-phonon coupling strength by using a localized surface plasmon (LSP) coupled to the emitter within the semiconductor. Previous work has demonstrated the possibility of producing coupled plasmon-exciton⁵ and plasmon-phonon⁶ modes. The exciton coupling is also influenced by the geometry of the structure due to the modification of the electromagnetic coupling in micro-cavities and can modify the radiative recombination process in nanostructures. There has, however, been no investigation to-date of whether these coupled modes can modify the electron-phonon and hole-phonon interactions within the semiconductor.

We present here evidence of modification of this coupling strength in InGaN/GaN QWs by the introduction of resonant plasmons to the system via metallic nanoparticles (NPs). The ability to induce localized SPs within a 2D quantum confined structure by infiltrating metal nanoparticles with InGaN QWs enables the modification of electron and hole-phonon interactions at the nanoscale limit. We provide direct experimental evidence of this change via observation of a collection-geometry forbidden Raman A₁ [transverse optical phonon or TO] mode. We also demonstrate that the introduction of metal NPs to the system also produces a significant change in the angle-dependence of the e/h-LOP coupling strength. Finally, we briefly discuss the possible origins of this change in the e/h-LOP interactions and the implications of the possibility of external modification of the coupling strength.

It has been demonstrated by members of our group that it is possible to incorporate metallic nanoparticles in the

^{a)} Author to whom correspondence should be addressed. Electronic mail: arup@unt.edu.

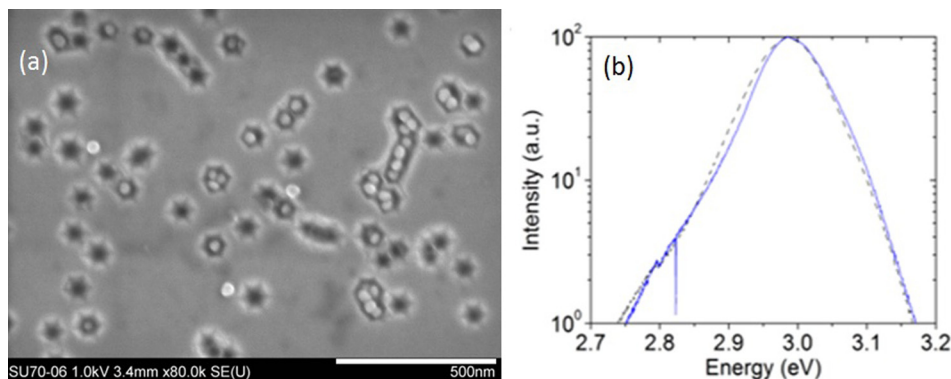


FIG. 1. (a) SEM images showing Ag NPs placed within the inverted hexagonal pits. (b) PL spectrum of the reference (black, dashed) vs. the Ag NP sample (blue) taken normal to the surface demonstrating the change in spectrum due to the NPs.

inverted hexagonal pits (IHPs) present in InGaN/GaN multi-QW (MQW) structures.⁷ These IHPs arise from threading dislocations (TDs) propagating from the GaN/sapphire interface^{8–11} and provide a simple and elegant location for placing metallic NPs within the QWs without affecting their structure.⁷ In this work, we have used a MQW structure which was grown via metal-organic chemical vapor deposition (MOCVD) on sapphire substrate and consists of 14-periods of 2.5 nm InGaN QWs separated by 7.5 nm GaN barriers. Two samples with this structure were grown, and one was infiltrated with Ag NPs with an average radius of 17 nm, while the other was left unaltered for use as a reference. The top down approach of infiltration of metal nanoparticles within quantum wells eliminates the possibility of any strain induced due to structural composition of the InGaN/GaN QWs. Characterization of the sample structure was performed via scanning electron microscopy (SEM) and atomic force microscopy (AFM). Figure 1 shows SEM of the sample structure with NPs embedded within the IHPs, along with the PL of the reference and Ag NP samples.

Raman excitation was provided by the 514 nm line of an Ar⁺ CW laser, and excitation and collection were along the c-axis of the sample with incident and scattered polarizations matched [c (a-a) \bar{c}]. A Horiba-T64000 UV-Visible Raman spectrometer was used for this experiment at room temperature. Figure 2 shows two important features resulting from

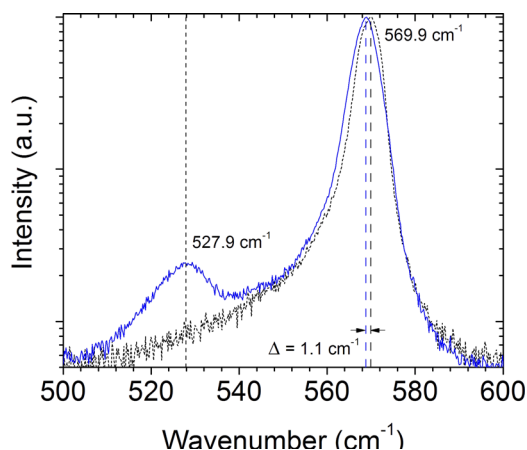


FIG. 2. Raman spectrum of the Reference (black, dashed) and Ag nanoparticles (blue) samples. The position of the $E_2(\text{high})$ and $A_1(\text{TO})$ phonons is marked for reference. Note that the $A_1(\text{TO})$ peak is absent in the reference measurement, and that the $E_2(\text{high})$ is shifted 1.1 cm^{-1} to the left for the Ag NP.

the addition of the NPs. First, the $E_2(\text{high})$ phonon peak (569.9 cm^{-1}) is shifted $\sim 1.1 \text{ cm}^{-1}$ to the left of the reference peak. We may exclude strain modification as a source of this observed Raman shift due to the top down approach for infiltration of the nanoparticles into the MQWs. Second, a second peak, corresponding to the $A_1(\text{TO})$ phonon, appears at 527.9 cm^{-1} . The second feature is particularly interesting, as the $A_1(\text{TO})$ phonon should not be observable using a [c (a-a) \bar{c}] excitation/collection geometry, but instead under [a (c-c) \bar{a}].¹² This suggests that the normal symmetries of e-ph coupling in GaN have been broken in the presence of the Ag NPs. Taken together these constitute significant experimental evidence of a change in the e/h-ph interactions within the system due to the presence of the Ag NPs.

The samples were also studied using angle-dependent PL (ADPL). The ADPL was performed using excitation from the 325-nm excitation from a HeCd laser, incident at -55° angle from the surface normal or the [0001] plane. Photoluminescence was then captured in 5° increments from 0° to 75° using a fiber-optic light guide and iris. The guide and iris were mounted on an arm attached to a goniometer centered beneath the sample. The normalized PL spectra at normal incidence are shown in Fig. 1(b). The measured spectra were then fitted using multiple Gaussians to extract the intensities of the PR using the model described in Ref. 13. Due to specular reflection of the excitation source, the fitting was not possible at 55° and 60° and hence the fitting results for those angles were discarded.

Figure 3 shows the angle-dependent intensity of the QW emission for the zero-phonon line, as well as the first and second phonon replicas. The intensities are normalized such that the sum of the intensities of the three components is unity at all angles. It is immediately obvious that there is a significant deviation in the intensities of the three components between the reference and Ag NP sample. This implies a modification of the e/h-LOP coupling within the InGaN/GaN quantum wells induced by the metal nanoparticles. The primary changes in the relative intensities occur for emission near normal and for emission around 45° . In the former case, the intensity of the first PR (1-PR) is decreased for the Ag NP sample relative to the reference. At 45° , on the other hand, the 1-PR emission is strongly increased relative to the reference sample.

Figure 4 summarizes these results in terms of the Huang-Rhys parameters (S_0 and S_1), which are direct measures of the strength of e/h-ph coupling in the system. The

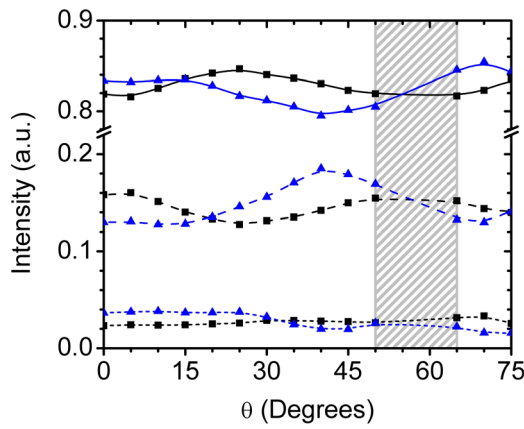


FIG. 3. Angle dependent PL intensity for the zero phonon, first (dashed), and second (dotted) phonon replicas of the InGaN/GaN MQWs with (blue) and without (black) Ag nanoparticles normalized with respect to the total emission (i.e., $I_{PR0} + I_{PR1} + I_{PR2} = 1$), where I_{PR0} , I_{PR1} , and I_{PR2} are the intensities of the zeroth, first, and second order phonon replicas, respectively. The gray shaded region represents missing values replaced by interpolation with a spline.

value of S_n has been determined empirically using the definition $S_n = (n+1)^{-1} I_{n+1}/I_n$.¹⁴ We have also measured the energy of the primary emission and the phonon replicas. As discussed previously,^{3,4} in InGaN, the phonon replicas are separated from the main peak by the energy of one or more LO phonons ($\hbar\omega_{LO} = 92$ meV). Since the distribution of phonons is not Gaussian, the peak of the first and second phonon replicas is offset from their expected positions by $1/2$ and $3/2$ kT, respectively, where $kT \sim 26$ meV at room temperature. In Figure 5, we show the differential energies of the three peaks measured as meV deviations from the reference emission energy of 2.984 eV. It is interesting to note that the first phonon replica energies line up well with the corrected phonon replica energy (horizontal dashed-dotted line: 80 meV (Ref. 8)). However, the second phonon replica lines up more closely with the uncorrected values (horizontal broken line: 184 meV (Ref. 14)). The surface plasmon energy of the Ag nanoparticles overlaps with the bandgap energy of the quantum well. However, there is no change in the absorption edge of the Ag-NP infiltrated InGaN QWs.

It is clear from the results above that there has been a modification in the relative intensities and emission energy of the zero-phonon line and the two phonon sidebands due to the presence of the Ag nanoparticles localized in the pits. This, in conjunction with the direct observation of a change in the symmetry of the Raman modes, presents compelling

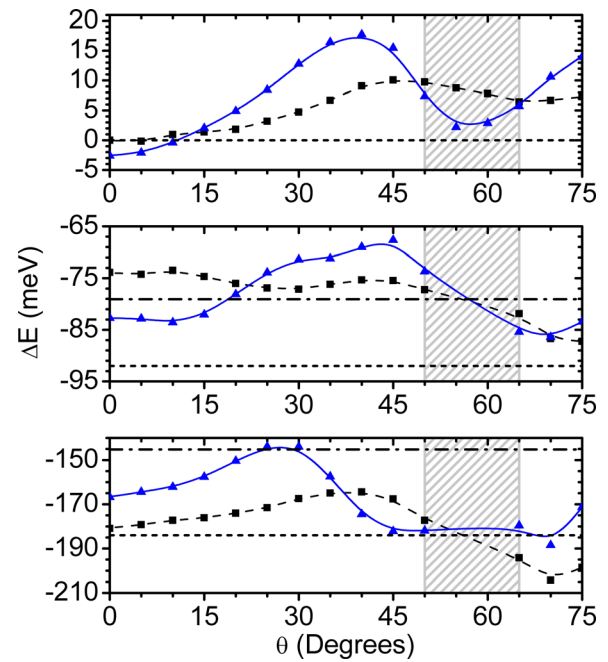


FIG. 5. (a) Emission energy of the main emission for reference (black squares), Ag (blue triangles) and measured as a deviation from the reference emission energy of 2.984 eV. (b) Emission energy of the 1st phonon replica. (c) Emission energy of the 2nd phonon replica.

evidence of modification of the e/h-ph interactions within the QWs. We discuss now two possible causes for the observed experimental results and possible experiments and modelling that may distinguish between the two effects.

The first possibility is that the modification is due to out-of-sample scattering of wave-guided modes by the Ag NPs. This is not an unreasonable assumption as the LSP energy is near-resonant to the emission energy of the QW, and so the Ag NPs should be able to scatter the light within the QW. Essentially, for scattering to explain the observed effects, there would need to be a significant anisotropy with respect to S and the emission direction. Such anisotropy clearly exists, as is evidenced in the angle dependence of S_0 and S_1 in the reference sample. This is due to the strong dependence of S on the phonon wave-vectors.¹⁵ Due to this anisotropy, photons emitted normal to the QW have a substantially different e/h-ph coupling than those emitted parallel to the QW. Mie scattering calculations, however, show that this is unlikely to be the reason for the observed results. Figure 6 shows the relative scattering intensity for s- and p-polarized light interacting with Ag NPs within an IHP.

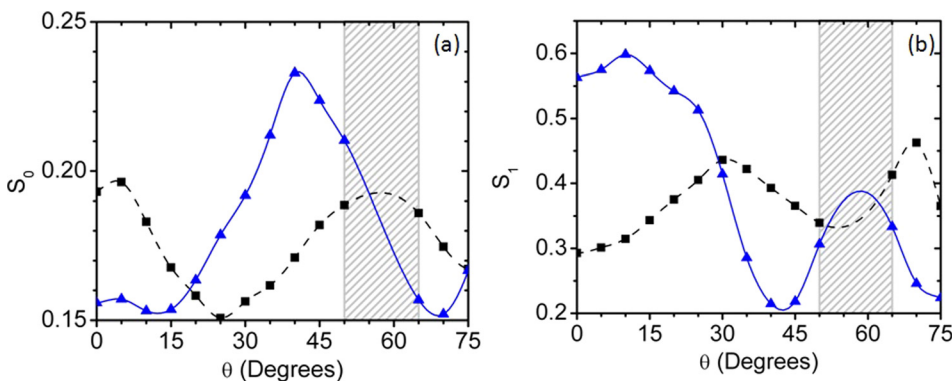


FIG. 4. The Huang Rhys parameters (a) S_0 and (b) S_1 as a function of emission angle for the reference (black squares) and Ag (blue triangles) system.

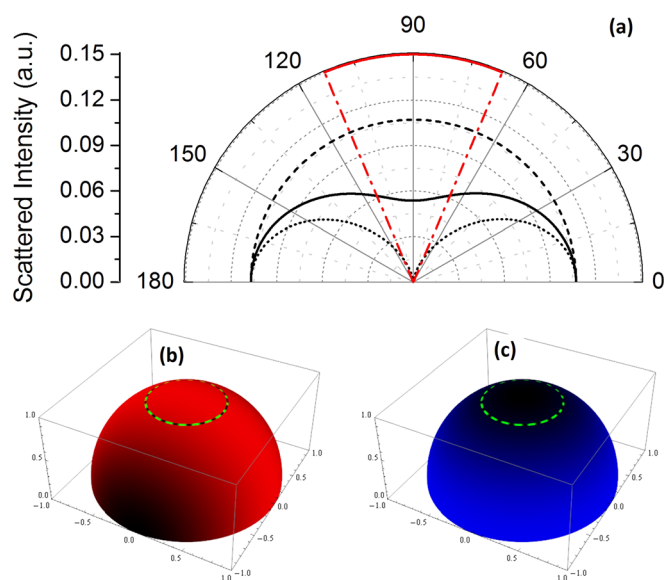


FIG. 6. (a) Simulated relative scattering intensity from a Ag nanoparticle within a GaN inverted heterostructure pit as a function of scattering angle for s polarized (dashed) and p polarized (dotted) light. Red cone represents the angles over which light is transmitted out. 3 D scattering pattern for (b) s polarized and (c) p polarized light from the same Ag NP. The dashed green circle represents the angles over which light can escape at the GaN/Air interface.

These calculations show that only 5% of the light scattered by the NPs will be scattered out-of-sample. Furthermore, the scattered emission is essentially entirely composed of s-polarized light and is isotropic, meaning that it cannot directly explain the changes in angle-dependence observed in the Ag NP sample. Additionally, neither the excitation source for the confocal Raman measurements nor the Raman scattered light is resonant to the Ag-NPs. This means that scattering by the Ag NPs cannot explain the appearance of the $A_1(\text{TO})$ mode in a forbidden geometry. Still, the Mie simulations only account for the situation where a single particle exists in a pit. It is possible that multiple particles per pit scatter wave-guided modes more strongly and maybe responsible for some of the observed angle-dependence.

The second, more interesting possibility is that the direct interaction between the plasmons and the carriers or the lattice is altering the electron-phonon coupling strength. Previous work has demonstrated the existence of coupled plasmon-exciton⁵ and plasmon-phonon modes.⁶ Although there is no prior investigation on the change of electron/hole-phonon (e/h-ph) coupling strength in the presence of these coupled modes, it is reasonable to expect that they should have a direct effect on the coupling strength. These coupled modes might also result in broken symmetry, allowing for the observation of the $A_1(\text{TO})$ mode in normally forbidden geometries.

Additional experiments may be able to better distinguish between these causes. Of primary interest would be confocal Raman measurements in $[a \text{ (c-c)} \bar{a}]$ and other geometries. Observation of other normally forbidden modes, Raman-inactive modes, or the mode being partially observable in multiple geometries may give clues as to how the symmetry of the system has been altered, and conclusively rule out scattering as a source. Furthermore, while the Raman measurements are non-resonant, the ADPL measurements are resonant to the system and may contain additional components from this resonant interaction. Angle-dependent electroluminescence would allow for separating out the effects due to resonant interaction between the excitation source from those due solely to interaction with the Ag NPs.

We have presented here strong evidence of modification of electron/hole-phonon coupling in InGaN/GaN MQWs by embedded Ag NPs. This effect is likely a result of plasmonic coupling to electron or phonon modes within the QWs. Due to the induction of phonon-replicas in the spectrum, the electron/hole-phonon coupling strength has a direct impact on the quality and efficiency of emission of the system; therefore understanding the source of this modification may provide an additional mechanism for using plasmonics to improve the internal quantum efficiency of light emitters. Furthermore, since phonon replicas exist in a many semiconductors, such a technique would be applicable over a wide range of light emitters.

¹N. Narendran and Y. Gu, *IEEE/OSA J. Disp. Technol.* **1**, 167 (2005).

²J. W. Lee, *J. Cryst. Growth* **315**, 263 (2011).

³M. Smith, J. Y. Lin, H. X. Jiang, A. Khan, Q. Chen, A. Salvador, A. Botchkarev, W. Kim, and H. Morkoc, *Appl. Phys. Lett.* **70**, 2882 (1997).

⁴P. Renwick, H. Tang, J. Bai, and T. Wang, *Appl. Phys. Lett.* **100**, 182105 (2012).

⁵N. T. Fofang, N. K. Grady, Z. Fan, A. O. Govorov, and N. J. Halas, *Nano Lett.* **11**, 1556 (2011).

⁶R. Kirste, S. Mohn, M. R. Wagner, J. S. Reparaz, and A. Hoffman, *Appl. Phys. Lett.* **101**, 041909 (2012).

⁷S. Pereira, M. A. Martins, T. Trindade, I. M. Watson, D. Zhu, and C. J. Humphreys, *Adv. Mater.* **20**, 1038 (2008).

⁸H. Morkoc, *Nitride Semiconductors and Devices* (Springer Verlag, Berlin, Germany, 1999).

⁹A. Neogi, H. Morkoc, T. Kawazoe, and M. Ohtsu, *Nano Lett.* **5**, 213 (2005).

¹⁰A. Hangleiter, F. Hitzel, C. Netzel, D. Fuhrmann, U. Rossow, G. Ade, and P. Hinze, *Phys. Rev. Lett.* **95**, 127402 (2005).

¹¹C. Netzel, H. Bremers, L. Hoffmann, D. Fuhrmann, U. Rossow, and A. Hangleiter, *Phys. Rev. B* **76**, 155322 (2007).

¹²A. G. Kontos, Y. S. Raptis, N. T. Pelekanos, and A. Georgakilas, *Phys. Rev. B* **72**, 155336 (2005).

¹³A. Llopis, J. Lin, S. Pereira, and A. Neogi, *IEEE J. Sel. Top. Quantum Electron.* **15**, 1400 (2009).

¹⁴R. Pecharroman Gallego, *Semicond. Sci. Technol.* **22**, 1276 (2007).

¹⁵X. B. Zhang, T. Taliercio, S. Kolliakos, and P. Lefebvre, *J. Phys.: Condens. Matter* **13**, 7053 (2001).